Spectrochimica Acta Part A: Molecular and Biomolecular Spectroscopy 105 (2013) 165–170

Contents lists available at SciVerse ScienceDirect

Spectrochimica Acta Part A: Molecular and Biomolecular Spectroscopy

journal homepage: www.elsevier.com/locate/saa

Naked Eye DNA detection: Synthesis, characterization and DNA binding studies of a novel azo-guanidine

Muhammad Jamil [a], Ataf Ali Altaf [b,c,*], Amin Badshah [b,*], Shafiqullah [b], Ibrar Ahmad [b], Muhammad Zubair [a], Saqib Kemal [b], Muhammad Irshad Ali [b]

[a] Department of Chemistry, Govt. College University Faisalabad, Pakistan
[b] Department of Chemistry, Quaid-i-Azam University, Islamabad 45321, Pakistan
[c] Department of Chemistry, University of Malakand, Chakdara, Dir (lower), Pakistan

HIGHLIGHTS

- A novel class of azo-guanidine compounds is introduced in this article.
- The compound (**AG**) interacts with DNA and gives clear color change in 70% ethanol.
- The **AG**–DNA complex was characterized with CV and UV–Visible spectroscopy.
- Electrostatic mode of interaction, and moderate binding constant ($K_b = 10^4$).
- Results indicate its potential use as DNA staining agent.

GRAPHICAL ABSTRACT

UV–Visible absorption spectra of 70 μM **AG** in the absence and presence of 20–140 μM DNA in 30% aqueous ethanol (30% H_2O:70% ethanol) buffer: 0.1 M phosphate buffer (pH 6.8), inset the visible picture of 70 μM **AG** in the absence (Left) and presence (Right) of 140 μM DNA in 30% aqueous ethanol (30% H_2O:70% ethanol) buffer: 0.1 M phosphate buffer (pH 6.8).

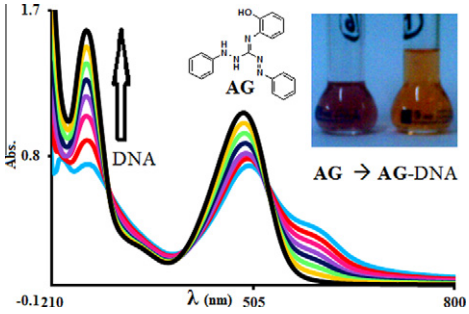

ARTICLE INFO

Article history:
Received 16 August 2012
Received in revised form 29 November 2012
Accepted 6 December 2012
Available online 20 December 2012

Keywords:
Azo-guanidine
DNA detection
DNA binding
Naked Eye DNA detection

ABSTRACT

A novel class of azo-guanidine compounds is introduced in this article. The novel compound 2-(2-hydroxyphenyl)-1-(phenylamino)-3-(phenylimino)guanidine (**AG**) was synthesized and well characterized by using different analytical instrumental techniques like elemental analysis, FTIR, ^{1}H and ^{13}C NMR, UV–Visible spectroscopy and cyclic voltammetry. The new compound was found interacting with DNA and shows clear color change in the solution. The **AG**–DNA complex was qualitatively and quantitatively characterized with UV–Visible spectroscopy and cyclic voltammetry. Electrostatic mode of interaction, clear color change and moderate binding constant ($K_b = 10^4$) indicate its potential use as DNA staining agent.

Introduction

The science of DNA sensing is always an open field of interest. It is important in exploring the inherited secrete of the nature of life. Huge numbers of chemical and/or instrumental methods are available for the DNA detection. The phenanthridium dye, ethidium bromide (**EtB**), is the stain that is most commonly used for directly detecting nucleic acids in electrophoretic gels [1]. This popularity

* Corresponding authors. Address: Department of Chemistry, Quaid-i-Azam University, Islamabad 45321, Pakistan (A. Badshah.). Tel.: +92 5190642131; fax: +92 512873869.
E-mail addresses: atafali_altaf@yahoo.com (A.A. Altaf), aminbadshah@yahoo.com (A. Badshah).

1386-1425/$ - see front matter © 2012 Elsevier B.V. All rights reserved.
http://dx.doi.org/10.1016/j.saa.2012.12.020

is due in part to the fact that, although unbound **EtB** has significant intrinsic fluorescence, the dye displays a 20–25-fold increase in fluorescence upon intercalation into double-stranded (ds) regions of nucleic acids [2]. **EtB** is used mainly in molecular biology laboratories. It is a suspected reproductive toxicant and exposure to it has the potential to negatively affect the human reproductive system. The severity and nature of the adverse effect is variable and can be influenced by factors such as sex, level of exposure and individual sensitivity to the chemical. It is thought to act as a mutagen because it intercalates ds-DNA, deforming the DNA and could affect DNA biological processes, like DNA replication and transcription [3–7]. The search for the alternatives is the keen interest of biochemist to avoid the use of **EtB**. Many other dyes have been reported in the past years to replace **EtB** and its adverse side affects for example SYBR, TOTO, YOYO families of dyes [8–10].

Among these dyes SYBR Green-I is considered to be the best and safe [1]. But in recent years, SYBR Green-I was found to be more mutagenic than **EtB** to the bacterial cells exposed to UV (which is used to visualize either dye) [7]. The more toxicity of SYBR Green I might be due to its stronger binding with DNA than **EtB** [11]. We consider the hypothesis, "weaker binding dyes with more observable change in any property would be the best and safe DNA sensing agent". In the present study we have synthesized a novel azo-guanidine dye and characterized its DNA binding behavior and binding constant using normally used instrumental techniques like cyclic voltammetry and UV–Visible spectroscopy [12–14].

Results and discussion

Synthesis

2-(2-Hydroxyphenyl)-1-(phenylamino)-3-(phenylimino)guanidine (**AG**) was synthesized by a well known literature reported *guanylation* method, our group have been reported many similar compounds using the same protocol [15–20]. **AG** was synthesized by the coupling of o-aminophenol and dithizone in the presence of Hg(II) and triethylamine in DMF (Scheme 1). Hg(II) reacts there to abstract sulfur while triethylamine capture HCl formed. The significant yield of **AG** shows the success of the protocol employed for the first time to synthesize such novel class of compounds (may be named as azo-guanidine). The synthesized compound was characterized in solid state by using FT-IR and elemental analysis as well as in solution phase using NMR and UV–Visible spectroscopy.

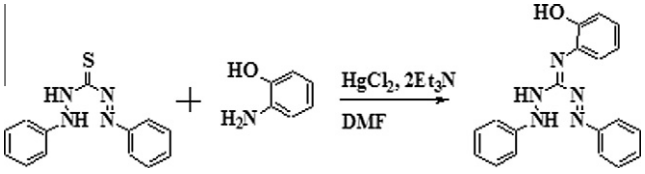

Scheme 1. Synthesis of 2-(2-hydroxyphenyl)-1-(phenylamino)-3-(phenylimino) guanidine (**AG**).

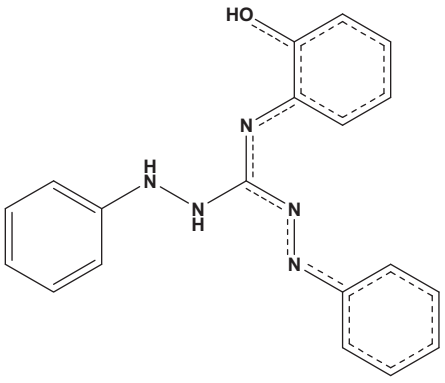

Fig. 1. The extended resonance in the **AG** structure.

The elemental analysis data shows that compound is highly pure and confined to the purposed structure in solid phase as the experimental elemental composition is in close agreement with calculated values. In infra-red spectroscopic characterization a sharp band at 3229 cm^{-1} was observed that indicates the presence of free hydrogen attached to nitrogen or oxygen (i.e. non H-bonded NH and OH groups). N═N of **AG** gives stretching band at 2358 cm^{-1}, C═N appears at 1736 cm^{-1}. These N═N and C═N bands shifted towards higher frequency than their normal absorption values might be originated from the extended conjugation in the structure (Fig. 1). While the other C—H, C—N and C—C bands appear in their characteristic regions.

Solution chemistry

AG is well characterized in solution phase (NMR, UV–Visible spectroscopy and electrochemical characterization with cyclic voltammetery) along with solid phase (elemental analysis and infra red spectroscopic) characterization. For solution phase characterization ^{1}H and ^{13}C NMR spectra were recorded in $CDCl_3$ and the data obtained is recorded in the experimental section. Signals at 2.904, 2.977 and 9.381 ppm may well be assigned to two NH and an OH proton while the other multiplet signal is originated from aromatic protons in the range of 7.142–7.806 ppm. In the ^{13}CNMR all the magnetically different carbons appeared at different positions. CN_3 carbon appears as most de-shielded carbon at 166.6 ppm and the carbon attached to the OH group appeared at 151.2 ppm.

In UV–Visible spectrum (Fig. 2), **AG** has three strong bands with high molar absorption coefficient (ε) in the range of 10500–11200 M^{-1} cm^{-1} at 222, 264 and 498 nm, a relatively low absorptivity (ε = 5728 M^{-1} cm^{-1}) band appeared at 570 nm as a shoulder. The high absorptivity bands in the UV-region of spectrum may confidently be assigned to the aromatic phenyl ring based π–π^* transitions, and N═N, C═N based π–π^* transitions.[21] In the visible region strong band at 498 nm with absorptivity (ε = 10571 M^{-1} cm^{-1}) can be attributed to the π–π^* transitions in the azo (N═N) group with highly extended conjugation over the seventeen atoms as shown in Fig. 1 and the shoulder at 570 may originated from n – π^* transitions in the azo (N═N) group [22].

The electrochemical properties of the present compound was investigated by CV on a glassy carbon electrode in 30% aqueous ethanol (30% H_2O:70% ethanol) 100 mV s^{-1}, supporting electrolyte: 0.1 M TBAP, in the concentration of 1×10^{-3} M vs. Standard Calomel Electrode (SCE). In the cathodic direction from +0.4 V to +0.65 V at scan rate of 100 mV s^{-1}, the CV of **AG** is characterized by one cathodic waves (at about 0.58 V) and flat line (no waves) in the anodic direction as depicted by cyclic voltammograms given in Fig. 2. No redox couple was observed in the voltamogram only a single oxidation peak observed in the CV graph as like most of the organic compounds. This oxidation peak may be originated from the oxidation of azo (N═N) group. The oxidation potential value is in agreement with the literature reported values of azo (N═N) group.[23,24] The appearance of only one oxidation peak indicates the irreversible electrochemical process [25].

DNA binding studies

Cyclic voltammeteric titration

The cyclic voltammetric behavior of **AG** in the absence and presence of 40 μM DNA at bare GCE is shown in Fig. 3. The voltammo-

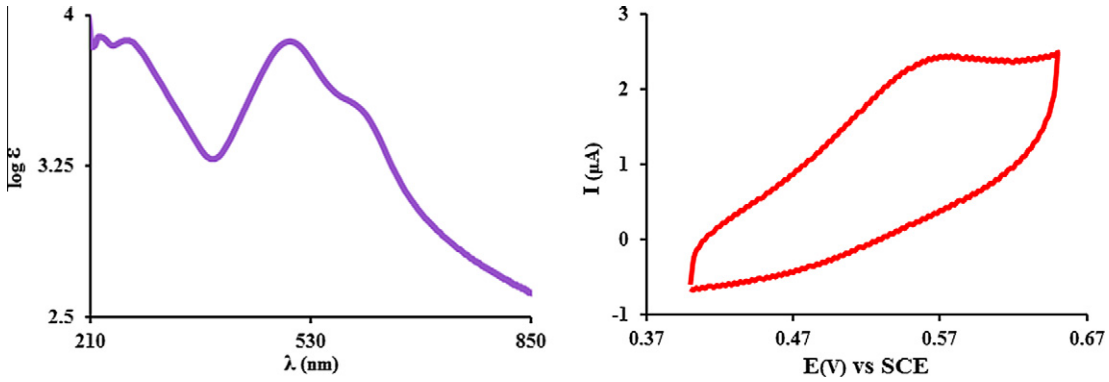

Fig. 2. (Left) UV–Visible absorption spectra of 70 μM **AG** in 30% aqueous ethanol (30% H_2O:70% ethanol); (Right) Cyclic voltammogram of 100 μM **AG** on a polished GC electrode in 30% aqueous ethanol (30% H_2O:70% ethanol) 100 mV s^{-1}, supporting electrolyte: 0.1 M TBAP.

gram without DNA (Fig. 2b) featured a well defined stable oxidation peak at the potential value of 0.578 V. By the addition of 40 μM DNA into 100 μM **AG** (Fig. 3) the cathodic peak potential (appeared at 0.536 V) was shifted by 42 mV in the negative going direction and I_{pa} was dropped by 21.4%. The substantial diminution in peak current is attributed to the formation of slowly diffusing **AG**–DNA supramolecular complex due to which the concentration of the free compound (mainly responsible for the transfer of current) is lowered. The mode of drug-DNA interaction can be judged from the variation in peak potential.

In general the positive shift (anodic shift) in formal potential is caused by the intercalation of the drug into the double helical structure of DNA, while negative shift is observed for the electrostatic interaction of the cationic drug DNA backbone [26]. So the obvious negative peak potential shift (cathodic shift) in the CV behavior of **AG** by the addition of DNA is attributable to the electrostatic interaction (H-bonding) between **AG** and the DNA. The cathodic peak potential shift further indicates that **AG** left over is easier to oxidize in the presence of negative environment of DNA. Because oxidized (**AG**$^+$) form is bound weakly to DNA than the reduced (neutral) form. As the ability of hydrogen bonding decreased on positively charging the compound in **AG**$^+$ state. Further addition of DNA diminishes the oxidation peak which supports the participation of **AG** in hydrogen bonding with DNA, and not let electrons to go out of the system (Fig. 4).

Based upon the decrease in peak current of **AG** by the addition of different concentration of DNA, the binding constants, K_b for the

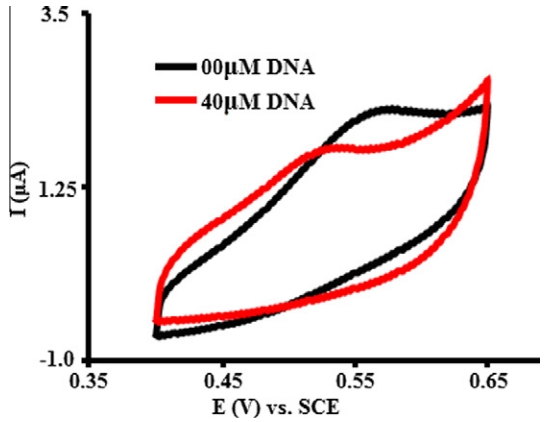

Fig. 3. Cyclic voltammograms of 100 μM **AG** in the absence and presence of 40 μM DNA on a polished GC electrode in 30% aqueous ethanol (30% H_2O:70% ethanol) 100 mV s^{-1}, buffer: 0.1 M phosphate buffer (pH 6.8), supporting electrolyte: 0.1 M TBAP.

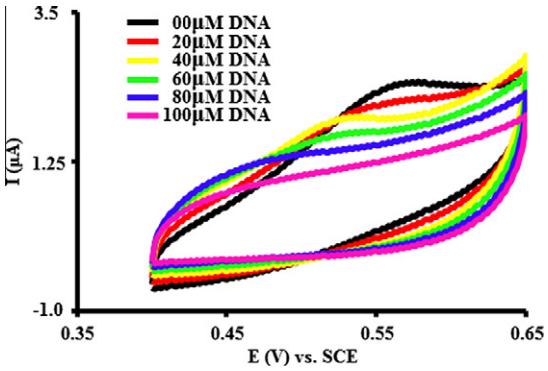

Fig. 4. Cyclic voltammograms of 100 μM **AG** in the absence and presence of 20–100 μM DNA on a polished GC electrode in 30% aqueous ethanol (30% H_2O:70% ethanol) 100 mV s^{-1}, buffer: 0.1 M phosphate buffer (pH 6.8), supporting electrolyte: 0.1 M TBAP.

AG–DNA complex formation were calculated according to the following Eq. (1) [25]:

$$I^2 = (I_o^2 - I^2)1/K_b[\mathrm{DNA}] + I_o^2 - [\mathrm{DNA}] \quad (1)$$

where K_b is the binding constant, I and I_o are the peak currents with and without DNA. A plot of I^2 vs. $(I_o^2 - I^2)$/[DNA] gave a straight line (Fig. 5a) with a slope equal to the reciprocal of binding constant, $K_b = 1.0 \times 10^4$ which is less than the binding constant of **EtB** (K_{EB} more than 10^5 M^{-1}) with DNA as reported in previous reports [27,28].

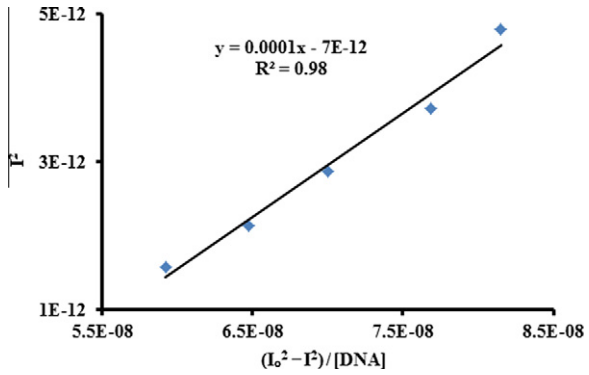

Fig. 5a. The plot of I^2 versus $(I_o^2 - I^2)$/[DNA] for the calculation of DNA binding constant from Cyclic voltammetric titration.

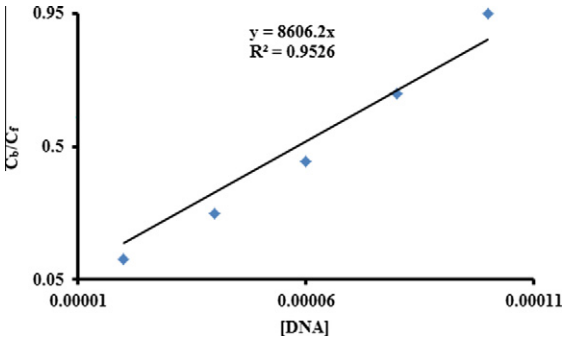

Fig. 5b. Plot of C_b/C_f versus DNA concentration for the calculation of the size of binding site.

For the determination of binding site size the following equation was used [29]:

$$C_b/C_f = K_b\,(\text{free base pairs})/s \tag{2}$$

where s is the binding site size in terms of base pairs (bp). Measuring the concentration of DNA in terms of base pairs concentration, the concentration of the base pairs can be expressed as [DNA]/2. So Eq. (2) can be written as:

$$C_b/C_f = K_b[\text{DNA}]/2s \tag{3}$$

C_f and C_b denote the concentration of the free and DNA bound species respectively. The C_b/C_f ratio was determined by the Eq. (4) given below [30]:

$$C_b/C_f = (I_o - I)/I \tag{4}$$

where I_o and I stands for the peak current of **AG** in the absence and presence of DNA, Putting the value of K_b as calculated according to above Eq. (1), the binding site size was obtained from the plot of C_b/C_f versus [DNA] (Fig. 5b). Putting the value of $K = 1.0 \times 10^4\ M^{-1}$ as calculated according to Eq. (1), the binding site size of 0.6 was obtained from the plot (Fig. 5b) of Cb/Cf versus [DNA]. The small value of s indicates electrostatic interaction of **AG** with DNA. Such an interaction may induce perturbation in the normal functioning of DNA which could presumably culminate in the prevention of replication and ultimate cell death [26].

UV–Visible spectrometric titration

The interaction of **AG** with DNA was also studied by UV–Visible absorption titration for getting further clues about the mode of

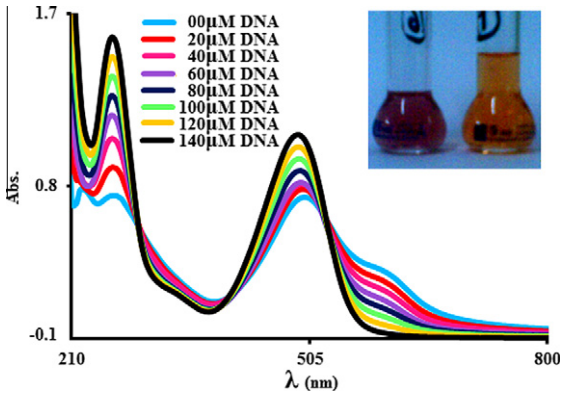

Fig. 6. UV–Visible absorption spectra of 70 μM **AG** in the absence and presence of 20–140 μM DNA in 30% aqueous ethanol (30% H_2O:70% ethanol) buffer: 0.1 M phosphate buffer (pH 6.8), inset the visible picture of 70 μM **AG** in the absence (Left) and presence (Right) of 140 μM DNA in 30% aqueous ethanol (30% H_2O:70% ethanol) buffer: 0.1 M phosphate buffer (pH 6.8).

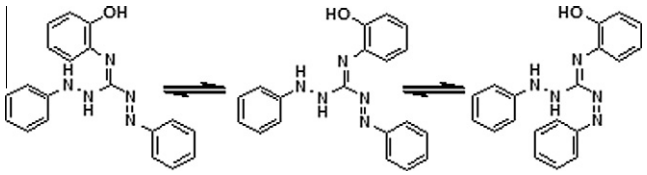

Scheme 2. Photoisomerization in **AG** many authors reported such kind photoisomerization in similar compounds [31–33].

interaction and binding strength. **AG** interacts with DNA and gives a clear color change visible with Naked Eye as shown in Fig. 6. UV–Visible spectroscopy is an effective tool for quantification of binding strength of DNA with small molecules. The effect of different concentration of DNA (20–140 μM) on the electronic absorption spectrum of 70 μM **AG** is shown in Fig. 6.

Different π–π^* and n–π^* transitions appeared in the UV–Visible spectrum of the compound, as discussed earlier. Upon interaction with DNA, **AG** reveals characteristic changes in the UV–Visible spectrum. In the spectral response of **AG** different type of changes occur after the addition of DNA. Both hypo and hyper chromic changes observed along with hypsochromic shift at 498 nm. There exist three isosbestic points (at 292, 402 and 526 nm) in the spectral picture of the **AG**–DNA reaction. The region below 300 nm is characteristic region of DNA where DNA nucleotides absorbs strongly, so the isosbestic point at 292 nm appears due to the increasing concentration of DNA which reveals the increasing absorbance in this region. The DNA interaction causes hypochromism above 526 nm and below 402 nm. The shoulder above 526 nm appears due to the azo based n–π^* transition which shows hypochromism after DNA interaction. This hypochromism may arise due to the hydrogen bonding of azo nitrogen with DNA and lone pair nitrogen becomes busy in the H-bonding and n–π^* transition depressed. As result of hydrogen bonding the molecule may become hindered molecule which increased the planarity of the molecule and stop the isomerism process shown in scheme 2 [31–33].

This planarity helps the penetration of AG into DNA strained structure which results in the expansion of helical structure of DNA. The planarity of the molecule also increase the chances of π-stacking which ultimately cause the hypsochromic shift of 10 nm in π–π^* transition. The maximum absorption of **AG** at this transition exhibited slight hypsochromic shift and pronounce hyperchromic shifts by the incremental addition of DNA. The expansion in the structure of either the compound alone and/or DNA after the formation of compound-DNA complex may result in hyperchromism. Hyperchromism of the same kind has also been reported by many other authors.[34–36] Based upon the decrease in absorbance at 570 nm and increase in absorbance at 498 nm the binding constant was calculated according to the following host guest Eq. (5) [37]:

$$\frac{A_o}{A - A_o} = \frac{\varepsilon_G}{\varepsilon_{H-G} - \varepsilon_G} + \frac{\varepsilon_G}{\varepsilon_{H-G} - \varepsilon_G}\frac{1}{K[\text{DNA}]} \tag{5}$$

where A_o and A are the absorbance of free compound and compound-DNA complex respectively, ε_G and ε_{H-G} is the molar extinction coefficients of free compound and compound-DNA complex respectively. The slope to intercept ratio of the plot $A_o/(A - A_o)$ versus 1/[DNA] yielded the binding constant Fig. 7, $K_b = 1.4 \times 10^4\ M^{-1}$, which is close to the value of K_b ($1 \times 10^4\ M^{-1}$) obtained from CV. The moderate binding constant is indicative of electrostatic interaction. The Gibbs energy change ($\Delta G = -RT\ \ln\ K_b$) of approximately −23.7 kJ/mol at 25 °C signifies the spontaneity of **AG**–DNA interaction. The binding behavior comparative data of **AG**, **EtB** and some other dyes given in Table 1 indicates that **AG** having the least bind-

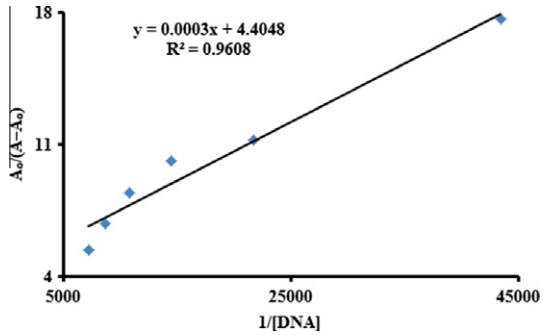

Fig. 7. The plot of $A_o/(A - A_o)$ versus 1/[DNA] for the calculation of DNA binding constant from UV–Visible spectroscopic titration.

Table 1
Comparative data of some normally used DNA staining agents and **AG**.

Sr. No.	Dye	DNA interaction mode	Binding constant (M^{-1})	Detection limit [40–44]	Ref.
1	**AG**	Electrostatic	10^4	15 ng/μL[b]	This work
2	**EtB**	Intercalation	$>10^5$	1 ng/μL	[27,28]
3	SYBR Green I	Groove binding	$>10^6$	60 pg/μL	[1,45]
4	TOTO-I	Intercalation	10^{-9}[a]	20 pg/μL	[46]
5	YOYO-I	Intercalation	$>10^{10}$	0.5 ng/μL	[47–49]
6	Methylene blue	Intercalation/ groove binding	$>10^4$	5 ng/μL	[27,50]

[a] The dissociation constant value.
[b] The detection limit calculated by the absorbance change at 484 and 604 nm wavelength.

ing constant and electrostatic mode of interaction might be the least toxic and the potential DNA detecting agent. As electrostatic interacting agents can cause just conformational changes in DNA and are less mutagenic than the intercalating agents [38,39].

Conclusion

In this paper, the synthesis, characterization and the DNA interaction of a noval azo-guanidine dye was comprehensively studied by spectrometry and electrochemical methods. The obvious hypochromic effect in absorption spectra and negative cathodic peak currant shifting suggested electrostatic binding mode between **AG** and DNA. The presence of isosbestic points in the UV–Visible spectroscopic behavior provides the evidence of the availability of two sites of interactions in the system. The strong color change in the visible picture of the reaction between **AG** and DNA provides the Naked Eye detection of DNA under the studied reaction conditions. These observations suggest the potential of **AG** as DNA staining agent. The binding constant data also suggesting, **AG** might be the better staining agent over normally used **EtB** due to weaker binding ability and clear color change [51]. Furthermore, the DNA staining agents like **EtB** cannot be used for the detection of DNA in ethanolic solution [52–55] whereas the novel **AG** will potentially do this job. Also the **AG** will be helpful for the quantification of DNA, as in the protocols used for the extraction of DNA, cold ethanol is used for the precipitation of DNA [56–59]. So the novel **AG** will be helpful for estimation of DNA move to the ethanol solution during precipitation. In future we are interested in the experimental toxicity, protein interaction and the other evolutions related to the use of **AG** as replacement of **EtB**.

Experimental

Materials

Mercuric chloride, dithizone, triethylamine, o-aminophenol, potassium dihydrogen phosphate, sodium hydroxide and Tetrabutylammoniumperchlorate were purchased from Sigma Aldrich. Deoxyribonucleic acid Sodium salt was purchased from acros organics. Solvents such as ethanol, DMF and methanol were purified before use according to the standard reported protocols [60,61]. Melting points were measured with BIO COTE Model SMP10 melting point apparatus. FT-IR and NMR spectra were obtained with Thermo Scientific Nicolet-6700 FT-IR and BRUKER AVANCE NMR spectrometer respectively.

Synthesis of 2-(2-hydroxyphenyl)-1-(phenylamino)-3-(phenylimino)guanidine (AG)

To the 50 ml DMF solution of 100 mmol dithizone, 100 mmol mercuric chloride were added with constant stirring in a round bottom flask fitted with reflux condenser, magnetic stirrer and hot plate. A 25 ml DMF solution of o-aminophenol (100 mmol) and triethylamine (200 mmol) were added drop wise to the dithizone and mercuric chloride solution. After complete addition the reaction mixture were refluxed for 6 h and extant of reaction were monitored on TLC. The reaction was completed with the formation black precipitates. The reaction mixture was filtered using sintered glass crucible. The solid crude product was then collected by pouring filtrate in ice cold water. The crude product was re-crystallized from hot methanol as crimson red fibrous crystals. Yield 78%; m.p 240–243 °C; Anal. Calc for $C_{19}H_{17}N_5O$: C, 68.87; H, 5.17; N, 21.13, Found C, 68.84; H, 5.15; N, 21.17%. FTIR (υ, cm^{-1}); 3229, 3048, 2358, 1736, 1654, 1592, 1524, 1494, 1455, 1434, 1349, 1269, 1189, 1132, 1069, 745, 676; UV–Visible λ_{max} (nm, (ε) $M^{-1}cm^{-1}$) 222 (11171), 264 (10685), 498 (10571), 570 (5728); ^{1}HNMR (300 MHz, ppm, δ); 2.904(bs, 1H), 2.977 (bs, 1H), 7.142–7.806 (*m*, 14H), 9.381 (bs, 1H); ^{13}CNMR (75 MHz, ppm, δ); 117.6 (2C), 122.3, 124.3, 126.1 (2C), 127.3, 128.0 (2C), 129.3, 129.5 (2C), 131.5, 136.4, 137.2, 138.1, 144.1, 151.2, 166.6 (CN_3).

Methods

DNA binding studies

Sodium salt of DNA was used as available from Acros Organics. Its stock solution was prepared by dissolving small amount in doubly distilled water. Concentration of DNA was measured spectrophotometerically by using 6600 M^{-1} cm^{-1} molar absorption coefficient at 260 nm. The DNA used was sufficiently pure and free from proteins evidenced from the ratio of absorbance at 260 and 280 nm (A260/A280 = 1.85) [62]. The system was buffered at pH = 7 by phosphate buffer (0.1 M KH_2PO_4 + 0.1 M NaOH). Stock solution was stored below 4 °C and used with in 4 days.

UV–Visible spectroscopy

Absorption spectra were measured on a UV–Visible spectrophotometer; Shimadzu 1800. The experiments involving the interaction of the compound **AG** with DNA were carried out in doubly distilled buffer (0.1 M KH2PO4 + 0.1 M NaOH, pH = 7) using 20% aqueous ethanol. The electronic spectrum of a known concentration of the **AG** was obtained without DNA. The spectroscopic response of the same amount of the **AG** was then monitored by varying the conc. of DNA. All of the samples were allowed to equilibrate for 5 min prior to every spectroscopic measurement [37].

Cyclic voltammetry

Voltammetric experiments were performed using EZstat-Pro Potential/ Galvanostatic of Nuvant System, Inc.USA. Measurements were carried out in a conventional three electrode cell which consisted of saturated calomel electrode (SCE) as a reference electrode, a thin Pt wire of thickness 0.5 mm with an exposed end of 10 mm as the counter electrode and a bare glassy carbon electrode (GCE) with a geometric area of 0.071 cm^2 as the working electrode. For electrochemical measurements TBAP was used as supporting electrolyte and the test solution was kept in an electrochemical cell (model K64 PARC) under constant temperature. The procedure was repeated for systems with constant concentration of **AG** and varying concentration of DNA at constant pH = 7. The working electrode was cleaned after every electrochemical assay.

Acknowledgment

Higher Education Commission, Islamabad, Pakistan is gratefully acknowledged for their support.

References

[1] V.L. Singer, T.E. Lawlor, S. Yue, Mutat. Res-Gen. Tox. Environ. 439 (1999) 37.
[2] J.B. Le-Pecq, C. Paoletti, Anal. Biochem. 17 (1966) 100.
[3] D. De-Medici, L. Croci, E. Delibato, S. Di Pasquale, E. Filetici, L. Toti, Appl. Environ. Microb. 69 (2003) 3456.
[4] N.V. Wurmb-Schwark, L. Cavelier, G. Cortopassi, Mutat. Res-Fund. Mol. Mech. 596 (2006) 57.
[5] G. Birkus, M.J.M. Hitchcock, T. Cihlar, Antimicrob. Agents Chemother. 46 (2002) 716.
[6] T. Storni, C. Ruedl, K. Schwarz, R.A. Schwendener, W.A. Renner, M.F. Bachmann, J. Immunol. 172 (2004) 1777.
[7] T. Ohta, S. Tokishita, H. Yamagata, Mutat. Res-Gen. Tox. Environ. 492 (2001) 91.
[8] B.N. Ames, J. McCann, E. Yamasaki, Mutat. Res. 31 (1975) 347.
[9] M. Fukunaga, B.A. Cox, R.S. von-Sprecken, L.W. Yielding, Mutat. Res-Fund. Mol. Mech. 127 (1984) 31.
[10] A. Larsson, C. Carlsson, M. Jonsson, B. Albinsson, J. Am. Chem. Soc. 116 (1994) 8459.
[11] V. Singer, X. Jin, D. Ryan, S. Yue, Biomed. Prod. 19 (1994) 68.
[12] M. Zaheer, A. Shah, Z. Akhter, R. Qureshi, B. Mirza, M. Tauseef, M. Bolte, Appl. Organomet. Chem. 25 (2011) 61.
[13] S. Niu, L. Hu, S. Zhang, J. Chem. Soc. Pakistan 29 (2011) 72.
[14] S. Zhang, S. Niu, G. Jie, K. Jiao, J. Chem. Soc. Pakistan 28 (2011) 33.
[15] G. Murtaza, A. Badshah, M. Said, H. Khan, A. Khan, S. Khan, S. Siddiq, M.I. Choudhary, J. Boudreau, F.G. Fontaine, Dalton Trans. 40 (2011) 9202.
[16] G. Murtaza, M.K. Rauf, A. Badshah, M. Ebihara, M. Said, M. Gielen, D. de-Vos, E. Dilshad, B. Mirza, Eur. J. Med. Chem. 48 (2011) 26.
[17] G. Murtaza, M. Ebihara, M. Said, M.K. Rauf, S. Anwar, Acta Crystallogr. E65 (2009) o2297.
[18] G. Murtaza, M.K. Rauf, M. Ebihara, A. Badshah, Acta Crystallogr. E65 (2009) o343.
[19] G. Murtaza, M. Said, M.K. Rauf, M. Ebihara, A. Badshah, Acta Crystallogr. E64 (2007) o333.
[20] G. Murtaza, M. Said, M.K. Rauf, M. Ebihara, A. Badshah, Acta Crystallogr. E63 (2007) o4664.
[21] D.L. Pavia, Introduction to Spectroscopy, Brooks-Cole Pub. Co., 2009.
[22] M.S. Masoud, A.E. Ali, M.A. Shaker, M.A. Ghani, Spectrochim. Acta A 60 (2004) 3155.
[23] M.M.M. Raposo, A.M.R.C. Sousa, A.M.C. Fonseca, G. Kirsch, Tetrahedron 61 (2005) 8249.
[24] M.M.M. Raposo, A.M.R.C. Sousa, A.M.C. Fonseca, G. Kirsch, Trans. Tech. Publ. (2006) 103.
[25] N. Arshad, U. Yunus, S. Razzque, M. Khan, S. Saleem, B. Mirza, N. Rashid, Eur. J. Med. Chem. 47 (2011) 452.
[26] A. Shah, M. Zaheer, R. Qureshi, Z. Akhter, M.F. Nazar, Spectrochim. Acta A 75 (2010) 1082.
[27] S. Nafisi, A.A. Saboury, N. Keramat, J.F. Neault, H.A. Tajmir-Riahi, J. Mol. Struct. 827 (2007) 35.
[28] W. Chen, N.J. Turro, D.A. Tomalia, Langmuir 16 (2000) 15.
[29] M.T. Carter, M. Rodriguez, A.J. Bard, J. Am. Chem. Soc. 111 (1989) 8901.
[30] M. Aslanoglu, C.J. Isaac, A. Houlton, B.R. Horrocks, Analyst 125 (2000) 1791.
[31] E.W.G. Diau, J. Phys. Chem. A 108 (2004) 950.
[32] T. Schultz, J. Quenneville, B. Levine, A. Toniolo, T.J. Martínez, S. Lochbrunner, M. Schmitt, J.P. Shaffer, M.Z. Zgierski, A. Stolow, J. Am. Chem. Soc. 125 (2003) 8098.
[33] A. Cembran, F. Bernardi, M. Garavelli, L. Gagliardi, G. Orlandi, J. Am. Chem. Soc. 126 (2004) 3234.
[34] A. Tarushi, G. Psomas, C.P. Raptopoulou, D.P. Kessissoglou, J. Inorg. Biochem. 103 (2009) 898.
[35] N. Shahabadi, M. Maghsudi, M. Mahdavi, M. Pourfoulad, DNA Cell Biol. 31 (2012) 122.
[36] Y.M. Chen, Y.J. Liu, Q. Li, K.Z. Wang, J. Inorg. Biochem. 103 (2009) 1395.
[37] F. Javed, A.A. Altaf, A. Badshah, M.N. Tahir, M. Siddiq, A. Shah, S. Ullah, B. Lal, J. Coord. Chem. 65 (2012) 969.
[38] A. Shah, R. Qureshi, A.M. Khan, R.A. Khera, F.L. Ansari, J. Braz. Chem. Soc. 21 (2010) 447.
[39] Z. Xu, G. Bai, C. Dong, Bioorg. Med. Chem. 13 (2005) 5694.
[40] S.R. Gallagher, P.R. Desjardins, Current Protocols in Human Genetics, 2007, A.3D. pp. 1.
[41] R.P. Haugland, Handbook of fluorescent probes and research products, Molecular Probes, 2002.
[42] J. Kapuscinski, Biotech. Histochem. 70 (1995) 220.
[43] http://www.sigmaaldrich.com/life-science/molecular-biology/nucleic-acid-electrophoresis/dyes-and-stains.html.
[44] H.S. Rye, S. Yue, D.E. Wemmer, M.A. Quesada, R.P. Haugland, R.A. Mathies, A.N. Glazer, Nucl. Acids Res. 20 (1992) 2803.
[45] S. Husale, W. Grange, M. Hegner, Single Mole. 3 (2002) 91.
[46] B.P. Bowen, J. Enderlein, N.W. Woodbury, Photochem. Photobiol. 78 (2003) 576.
[47] A. Sischka, K. Toensing, R. Eckel, S.D. Wilking, N. Sewald, R. Ros, D. Anselmetti, Biophys. J. 88 (2005) 404.
[48] A.N. Glazer, H.S. Rye, Nature 359 (1992) 859.
[49] L.M. Wilhelmsson, N. Kingi, J. Bergman, J. Med. Chem. 51 (2008) 7744.
[50] R. Rohs, H. Sklenar, J. Biomol. Struct. Dyn. 21 (2004) 699.
[51] Q. Huang, W.L. Fu, Clin. Chem. Lab. Med. 43 (2005) 841.
[52] C.R. Merril, Gel Staining Techniques, eLS, 2005.
[53] B.J. Bassam, G. Caetano-Anolles, P.M. Gresshoff, Anal. Biochem. 196 (1991) 80.
[54] R.P. Haugland, M.T.Z. Spence, I.D. Johnson, The handbook: a guide to fluorescent probes and labeling technologies, Molecular Probes, 2005.
[55] C. Ding, C.R. Cantor, J. Biochem. Mol. Biol. 37 (2004) 1.
[56] A. Böhm, D. Bartel, N.U. Szucsich, G. Pass, Soil Organ. 83 (2011) 335.
[57] A. Rodríguez, M. Rodríguez, M.I. Luque, A.F. Justesen, J.J. Córdoba, Food Control 25 (2012) 666.
[58] K.L. Cook, L.B. Hill, Development of in-house methods for high-throughput DNA extraction, in: Kentucky Water Resources Annual, Symposium, 2012, pp. 25.
[59] S. Bonin, P.J.T.A. Groenen, I. Halbwedl, H.H. Popper, Guidelines Mole. Anal. Arch. Tissues (2011) 37.
[60] P.J. Alaimo, D.W. Peters, J. Arnold, R.G. Bergman, J. Chem. Educ. 78 (2001) 64.
[61] J.A. Glass, Solvent Purification by Distillation with a Hydrocarbon Oil, Google Patents, 1969.
[62] S.A. Bailey, D.E. Graves, R. Rill, G. Marsch, Biochemistry 32 (1993) 5881.